



## Extracting metals from aqueous solutions using Ti-based nanostructures: a review

Francisco Jose Alguacil, Felix Antonio Lopez, Irene Garcia-Diaz\*

*Centro Nacional de Investigaciones Metalúrgicas (CSIC), Avda. Gregorio del Amo 8, Madrid 28040, Spain, emails: fjalgua@cenim.csic.es (F.J. Alguacil), flopez@cenim.csic.es (F.A. Lopez), Tel. +34 915538900; Fax: +34 915347425; email: irenegd@cenim.csic.es (I. Garcia-Diaz)*

Received 20 March 2015; Accepted 12 August 2015

### ABSTRACT

Titanium-based nanostructures due to their special physicochemical properties are receiving a great deal of interest for their applications in several fields. Among these applications, the various Ti-based nanostructures are finding their value as “green adsorbents” or ion exchangers for metals present in aqueous solutions arising from various environments. The present paper reviewed significant applications of these amazing materials in the removal of metals from heavy to radioactive ones.

*Keywords:* Titanium-based nanostructures; Adsorption–desorption–regeneration; Metals; Liquid effluents

### 1. Introduction

#### 1.1. Preparation of titanium-based nanostructures

Beneficial aspects of nanotechnology have attracted great attention toward the synthesis and application of nanomaterials. Titanate nanomaterials (TNMs) have become a major concern because of their unique properties, such as large specific surface area, good structural stability, and ion-exchange capability [1–3]. Generally, TNMs refer to titanate nanotubes (TNTs) [1], titanate nanosheets (TNSs) [4], titanate nanorods [5], titanate nanowires [6], titanate nanobelts [7], and so on.

Until now, the only precursor used to prepare the various forms of titanium-based nanostructures is  $\text{TiO}_2$ , though some titanium nanostructures serve themselves as precursors of other ones, furthermore

and broadly speaking, all these various nanostructures are prepared by an alkaline hydrothermal processing of titanium(IV) oxide by a process dated back in 1998 [8,9]. A couple of years before, it was reported the procedure to obtain  $\text{TiO}_2$ -based nanotubes via an electrochemical deposition in a porous aluminum oxide mold, and in 1999 the electrochemical anodic oxidation technique was used to produce titanium-based nanotubes [10].

As it is mentioned above, the first description of how TNTs were obtained by a hydrothermal process in alkaline media dated back to 1998. In the process, anatase powders were chemically treated with 5–10 M NaOH solutions during 20 h at 110 °C. The as-obtained nanotubes presented a specific surface as high as near 400  $\text{m}^2/\text{g}$  [8]. This type of treatment was constantly repeated in all the literature consulted in this review.

The growth of the nanostructures during the hydrothermal process follows 3D, 2D, 1D mechanism

\*Corresponding author.

[11]. The raw  $\text{TiO}_2$  precursor is first transformed into 2D lamellar structures and then roll to form 1D structures.

It is doubtless that the synthesis conditions (hydrothermal temperature, the concentration of reactants, the hydrothermal duration) and the post-treatment (washing times, acid concentration, and the sequence of washing by solvent and acid, post heat-treatment) are crucial parameters that affect the structures (crystallography and morphology) and physical-chemical properties of the products in the synthesis of TMN materials by hydrothermal method [12–20].

Some studies reported the effect of alkaline type and concentration on the formation and transformation of titanate microstructures [21–25]. In general, the morphologies of the titanate products were determined by the reaction conditions, especially the concentration of alkali, generally NaOH [25]. Various TNMs were synthesized by  $\text{TiO}_2$  nanoparticles (90% anatase and 10% rutile) via hydrothermal reaction ( $T^\circ = 130^\circ\text{C}$  for 72 h) under different NaOH concentrations (4–15 M). The Morphology of TNMs successively exhibited as nanogranules ( $C_{\text{NaOH}} = 4\text{ M}$ ), nanoplates ( $C_{\text{NaOH}} = 5\text{ M}$ ), nanotubes are began to form when a concentration of 7 M coexisted with nanosheets, with a concentration of 10 M the nanotubes are obtained, these present a long length of hundred nanometers. Nanosheets are obtained to a NaOH concentration of 12 M and nano-blocks to higher NaOH concentration, 15 M [26]. Huang et al. [25] research also the effect of the NaOH concentration (3–15 M) on the formation of TNMs by hydrothermal method treating anatase at  $180^\circ\text{C}$  for 24 h. Under the different concentrations of NaOH, 3, 5, 10, 12, and 15 M the products obtained were nanosheets, nanotubes, an admixture of nanotubes and nanowires, nanowires and amorphous particles, respectively. The structure of both nanosheets and nanotubes can be identified as  $\text{Na}_2\text{Ti}_2\text{O}_5 \cdot 2\text{H}_2\text{O}$ , while the crystal structure of nanowires is in agreement with  $\text{NaTi}_2\text{O}_4 \cdot \text{OH}$ .

If the precursor reacts with solutions of NaOH concentrations below 5 M, the titanate-based nanostructure formed is nanoflowers. The decrease in alkaline concentration may also result in a slower rate of nanosheets scrolling, the lamellar structures cannot roll into 1D structures due to the thickness of nanosheets growing faster than the width of it, and by this reason, the nanosheets are too rigid to bend before curving occurs. As a result, the sheet curled to thin curled flakes. The flakes did not complete separate so its looks like a flower [27].

If the alkaline precursor in the hydrothermally treated is KOH solutions with a concentration of 4–25 M not tubular structure are produced but

wire-like products are obtained. Also, the hydrothermal treating of  $\text{TiO}_2$  powders with LiOH solution leads to the formation of nanoparticles only [1]. A binary mixture containing KOH and NaOH concentrated could reduce the hydrothermal temperature on the formation of TNTs [28]. The molar ratio  $\text{TiO}_2/\text{NaOH}$  can also affect the diameter of the nanotubes [17,22].

The reaction time can also affect the structure of the TMNs, the production of nanotubes increase with prolonged duration of hydrothermal treatment, although prolonged duration might lead to the transformation from nanotubes to nanofibers [29]. Yoshida et al. [18] prepared nanotubes by hydrothermal synthesis from  $\text{TiO}_2$  powder as a starting material and 10 M NaOH at  $120^\circ\text{C}$  for a reaction time 6–72 h. Under the synthesis conditions, at all reaction times, nanotubes were obtained. The nanotubes became long until 12 h. At 12 h or more, the structure of the nanotubes was not obviously changed, maybe due to the fineness of the starting powder and rather the low reaction temperature. The nanotubes prepared from a reaction time of 12 h have diameter of 10 nm and specific surface areas of  $300\text{ m}^2/\text{g}$ .

However, different only titanate-based nanostructures can be isolated by variation of the sodium hydroxide concentration and the reaction time at a fixed temperature of  $180^\circ\text{C}$ . When the  $\text{TiO}_2$  precursor is treated during 2 h with 5–12 M NaOH solutions, nanosheets with  $\text{Na}_2\text{Ti}_2\text{O}_5 \cdot \text{H}_2\text{O}$  stoichiometry are formed. An increasing in the treatment duration to 4 h, transformed the first structure, nanosheets, to nanotubes with orthorhombic  $\text{Na}_2\text{Ti}_2\text{O}_5 \cdot \text{H}_2\text{O}$  composition, if the treatment is prolonged to 6 h, nanowires with monoclinic  $\text{NaTi}_2\text{O}_4(\text{OH})$  structure begin to form, formation which is completed after 12 h of treatment [25]. On the other hand, at  $130^\circ\text{C}$  and time reaction of 12 h, many thin sheets and some nanotubes coexist, at 24 h many nanotubes and few thin sheets are observed. After 36 h, almost all the products are nanotubes [30]. Sreekantan and Wei [22] observed at temperatures of  $150^\circ\text{C}$ , 15 h are enough for complete conversion of titania nanoparticles to nanotubes.

Different titanate nanostructure composites can be formed at various temperatures; thus, when the hydrothermal temperature increases from 60 to  $230^\circ\text{C}$ , the various structures formed are: nanoparticles, nanosheets, nanotubes, nanowires, nanoribbons, and nanorods, see Table 1 [23,31–36]. Huang et al. [37] demonstrated that the variation of the temperature only results in the acceleration of the kinetic reaction rate and does not determine the morphology of the end nanostructure.

The post-treatment of the titanium-based nanostructures had found in order to investigate their

Table 1  
Effect of the temperature in the titanate nanostructures

Refs.	T°	Nanostructures
[23,25,33,34]	60–100	Nanosheets
	100–180	Nanotubes
	>180	Nanowires
[31,32]	180–250	Nanoribbons
[33]	100	Sodium titanate nanoparticles
	125	Nanotubes
	>180	Nanorods
[35]	120	Nanotubes
	150	Nanowires
[36]	110–160	Nanotubes
	>160	Nanorods

structure and properties. It was also described that the acid washing of layered TNTs played an important role in controlling the amount of Na<sup>+</sup> remaining in the TNTs, Na<sub>x</sub>H<sub>2-x</sub>Ti<sub>3</sub>O<sub>7</sub>·nH<sub>2</sub>O, leads to the substitution of Na<sup>+</sup> for H<sup>+</sup>, modifying the structure and properties of the substituted nanocompound [38].

Lee et al. [39] studied the effect of washing with 0.1–0.001 M HCl solution and distilled water the TNTs after the hydrothermal process. In samples washed with 0.01 and 0.001 M HCl, a large amount of nanotubes of which formula may be Na<sub>x</sub>H<sub>2-x</sub>Ti<sub>3</sub>O<sub>7</sub>, with a diameter of 10–30 nm and a length of several hundreds of nanometers, are obtained. However, the nanotubular structure of sample washed with 0.1 M HCl becomes diffuse and the lengths of the TNTs become short. When the sodium content of TNT is approximately 0 wt% (nearly complete proton exchange), the nanotubular structure of titanates may be destroyed. Moreover, it has been reported that for TNT sample with low sodium content (such as 1.2 wt%), the TNTs were essentially a protonic layered titanate and the structure was very close to H<sub>2</sub>Ti<sub>3</sub>O<sub>7</sub> [40]. Liu et al. [41] studied the effect of different washing treatment. A washing with 0.1 M NaCl aqueous solution mainly resulted in TNSs while treating with deionized water or 0.1 M HCl (pH > 7) aqueous solution can obtain highly crystallized TNTs. If the pH after acid washing processes were below 7, trace of nanotubes can be found, but almost all of them were damaged.

The temperature variation in the post heat-treatment of nanomaterials may be affected in the structure and the stability of these [42].

There are no significant differences in the physical appearance of TNTs before and after annealing (400°C for 2 h). This suggests that the annealing under this condition does not damage the tubular structure of the sample [43,44]. However, the measured Bet Surface area and pore volume in the annealing TNTs

samples show a decrease, Sp and Vt of TNTs is 448.4 m<sup>2</sup>/g, and 1.3 cm<sup>3</sup>/g to the annealed titanotubes these values are 128.1 and 1.0 m<sup>2</sup>/g, respectively. Zhao et al. [45] annealed titania nanotubes at 500°C for 3 h, the Bet area was 121.2 m<sup>2</sup>/g, Peng et al. [46] reported the BET surface area of TNTs at 450°C 2 h was 149.6 m<sup>2</sup>/g.

The post heat-treatment of nanotubes synthesized at 120°C for 72 h, during 2 h at temperatures between 100 and 600°C was studied by Yoshida et al. [35]. Apparently, the samples treatment for 2 h at 100, 200, and 300 are composed by nanotubes and not changed their microstructure drastically; however, a slight decrease in the interlayer spacing with the increase of the temperature is observed. However, the nanotubes microstructure were destroyed and changed into particles when the samples were heated for 2 h at temperatures higher than 350°C. The nanotubes, with less Na<sup>+</sup>, began to be destroyed and became into anatase-type TiO<sub>2</sub> particles and the others of the nanotubes remain as the nanotubes where a lot of Na exist, indicating the remnant Na stabilized nanotubes structures. At higher heat-treatment temperatures (650–900°C), the particles change into rutile phase and the nanotubes change into solid nanorods of Na<sub>2</sub>Ti<sub>6</sub>O<sub>13</sub>.

## 2. Titanate-based nanomaterials as adsorbents of metals from aqueous solutions

One-dimensional carbon-titanate nanomaterials composites: particles, sheets, tubes, wires, and ribbons, presented good properties against the adsorption of Cu<sup>2+</sup> and Pb<sup>2+</sup> from aqueous solutions [47]. The maximum metal uptake for the above nanostructures is in the 1.3–2.0 and 0.9–2.8 mmol/g ranges for copper(II) and lead(II), respectively.

CS<sub>2</sub>-modified TNTs were used for the adsorption of copper(II), lead(II), and silver(I) presented in water [48]. The adsorption capacity seemed to be related with the accompanying anion and the pH value of the aqueous solution, being the adsorption capacity of the modified nanotubes better than that of the raw TNTs (Table 2) in the case of lead(II), worse in the case of silver(I) and practically constant in the case of copper(II).

TNTs prepared via a hydrothermal treatment of titanium(IV) oxide powders in a 10 M sodium hydroxide medium and 150°C during 24 h were used for the removal of copper(II) from aqueous solutions [49]. The adsorption capacity of the nanotubes depends on the amount of Na<sup>+</sup> in the nanotube; if this presence is not very low (i.e. higher than 7.2 wt%), the nanotubes are good adsorbents of copper(II) with a maximum capacity of near 1.9 mmol/g at a pH value of 5. With an

Table 2

Comparison of metals adsorption capacity of unmodified and CS<sub>2</sub>-modified TNTs [48]

Nanotube	Metal	Anion	pH	Adsorption capacity (mmol/g)
Unmodified	Pb(II)	Acetate	5.2	2.9
	Cu(II)	Chloride	4.0	1.8
	Cu(II)	Acetate	5.1	2.6
	Ag(I)	Nitrate	7.3	4.4
CS <sub>2</sub> -modified	Pb(II)	Acetate	5.0	3.2
	Cu(II)	Chloride	3.2	1.5
	Cu(II)	Acetate	5.0	2.5
	Ag(I)	Nitrate	7.2	3.9

endothermic adsorption process, the adsorption of copper(II) is well described with the Langmuir model:

$$Q_e = \frac{Q_{\max} b C_e}{1 + b C_e} \quad (1)$$

where  $Q_e$  (mmol/g) is the adsorption capacity at equilibrium,  $C_e$  (mmol/L) is the concentration of the metal in the solution at equilibrium,  $Q_{\max}$  (mmol/g) is the maximum metal uptake of the adsorbent, and  $b$  (L/mmol) is the Langmuir constant related to the affinity of binding sites and it is also a measure of free energy of adsorption. The adsorption kinetics followed the pseudo-second-order model:

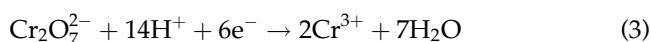
$$\frac{t}{Q_t} = \frac{1}{k_2 Q_e^2} + \frac{t}{Q_e} \quad (2)$$

where  $Q_t$  and  $Q_e$  are the amount of metal adsorbed at an elapsed time and at equilibrium, respectively, and  $k_2$  is the second-order rate constant. Experimental data concluded that the controlling process is attributed to the aqueous diffusion.

Arsenic, in its two stable oxidation states (III) and (V) in aqueous solution, is one of the most toxic elements; thus, its removal from aqueous solutions is a general concern. TNTs were among the many adsorbents investigated for their use in this field [50], and whereas As(V) is mainly adsorbed at acidic pHs values, As(III) is best removed from aqueous solutions at pH around 7 using these nanoadsorbents. In any case, the temperature in which the nanotubes are formed influences the arsenic uptake as results in Table 3 showed, and is far greater than that obtained by the use of titanium oxide powders.

The maximum capacity of As(III) and (V) obtained by the Langmuir model is 0.8 and 2.8 mmol/g, respectively, and both can be desorbed from loaded TNTs by the use of sodium hydroxide solutions, with desorption yields of 95% for arsenic(V) and 85% for arsenic(III).

Two types of TiO<sub>2</sub> nanostructures were used for the reduction of chromium(VI) presented in aqueous solution [51]. The titanium-based nanostructures used in the investigation were TiO<sub>2</sub> nanofibers and TiO<sub>2</sub> nanoparticles, where the nanofibers were used as precursors of various types of nanoparticles. Results obtained from this study showed that the elimination of chromium(VI), from an aqueous solution of pH 2.5, is best performed using TiO<sub>2</sub> nanoparticles (75% metal removal after 180 min) if compared with that of the nanofibers (32% in the same period time), though chromium(VI) reduction efficiency is pH dependent, being this removal higher as the pH of the solution is decreasing. The removal of chromium(VI) is carried out upon UV irradiation, being the overall photocatalytic reaction described as:



The photoreduction of chromium(VI) was also investigated by the use of WO<sub>2</sub> doped TiO<sub>2</sub>-nanotubes but in the presence of citric acid [52]. This acid plays a definite role in the reduction process since it acts as an electron-donor and it takes part in the reaction under UV light. The pH of the solution is also a key-variable to improve the reduction of chromium(VI), since this is increased as the pH of the solution decreased (i.e. near quantitative chromium(VI) removal at pH 1 and 60 min against near 2–5% removal at pH 7 and the same elapsed time). Strangely, in this work, there is a terrible mistake since in most of the figures, chromium is erroneously captioned as Cr<sup>6+</sup> when this element in the oxidation state of VI never exists as a cation.

Solutions containing Cr(III) and Cr(VI) were subjected to the simultaneous metal adsorption with mixture of TiO<sub>2</sub> and TNTs [53]. The process is well conducted at pH of 5, and consists of a single step in which chromium(III) is transferred from the TiO<sub>2</sub>

Table 3  
As(III) and (V) adsorption using various TNTs [50]

Temperature of formation (°C)	As(III) (mmol/g)	As(V) (mmol/g)
110	0.08	0.08
180	0.11	0.13

Notes: Time: 300 min The adsorption using the pristine titanium oxide powder is 0.02 and 0.03 mmol/g for arsenic (III) and (V), respectively.

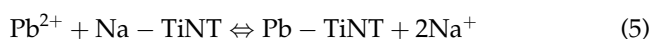
surface to the TNTs interlayers, process which greatly promoted the release of photocatalytic activity of the nanotubes by inhibiting electron–hole pairs recombination; moreover, the presence of calcium(II) ions benefit photocatalysis due to the formation of bridges  $-\text{TiOH}^+-\text{HCrO}_4^--\text{Ca}^{2+}-\text{HCrO}_4^-$ .

Titanate whiskers were used to the adsorption of Cu(II), Pb(II), and Cr(III) [54]. Titanate whiskers with formula,  $\text{H}_{2-x}\text{K}_x\text{Ti}_3\text{O}_7$ , were prepared by autoclaving metatitanic acid at 150°C for 18 h to obtain anatase which react by hydrolysis, at 140° for 48 h, with a concentration of 4–12 M KOH, then part of the samples was washed with distilled water and other part was washed with HCl (0.1 M). The samples washed with water present an  $x$  value of 0.6; however, in the samples washing with HCl the potassium content diminish, the hydrochloric acid cause the ion exchange between protons and potassium ions,  $x = 0.3$ , with a decrease in the layer distance. In all the cases, the surfaces areas are ranged between 245.0 and 382.0 m<sup>2</sup>/g. Cu(II), Pb(II), and Cr(III) ions are rapidly adsorbed on the surfaces of titanate whisker, in 30 min. At 150 min, the maximum adsorption capacities are 2.2, 1.9, and 1.9 mmol/g, respectively, when the initial concentrations are 150, 300, and 80 mg/L. The adsorption is affected by the ion exchange of metals ions with K<sup>+</sup>. The whiskers present a pseudo-second-order adsorption kinetics. The Langmuir adsorption isotherms are well fitted to Cu(II) and Pb(II) with a maximum adsorption capacity of 2.3 and 1.9 mmol/g, respectively, while the Freundlich adsorption equation is well fitted for the adsorption of Cr(III) by titanate whiskers.

Chang et al. [55] study the influences of lignosulfonate on the structure and adsorption capacity of Pb(II), Cu(II), and Cd(II) onto TNTs. The layer spacing and crystallinity on the lignosulfonate-TNTs (L-TNTs) is higher than TNTs, the layer spacing calculated from the Bragg formula is 0.96 and 0.69 nm, respectively. The surface area of L-TNTs (229 m<sup>2</sup>/g) is lower than that of TNTs (247 m<sup>2</sup>/g), this may be due to the partial occupation of the surface by lignosulfonate adsorbed. Langmuir monolayer adsorption model is

described to the adsorption isotherms of L-TNTs for Pb(II), Cu(II), and Cd(II). The maximum adsorption capacities are 3.6, 2.0, and 2.3 mmol/g for Pb(II), Cd(II), and Cu(II), these values are higher than those of TNTs.

It is described that in the adsorption of lead(II) using TNTs [56], the metal adsorption onto the nanotubes is mainly attributed to exchange with sodium ions and binding with the oxygen atoms on the nanotubes surface:



In this investigation, it is also found that high lead loadings onto the nanotubes, as much as near 1.0 mmol Pb(II)/g adsorbent, can be achieved at pH values of 5–6, and that the microwave intensity and energy used in the hydrothermal preparation of the nanotubes did not affect linearly with the adsorption capacity of the adsorbents. With respect to the influence of the pH value on the metal adsorption, its influence is resumed in Table 4; it can be seen that the adsorption decreased with the decrease of the pH value.

An important step after adsorption is separation of the spent adsorbent for the treated water, which is conventionally performed by filtration or centrifugation [57]. Recently, spinel ferrite nanoparticles have attracted considerable interest owing to their excellent magnetic properties. Among such nanoparticles, cobalt ferrite (CoFe<sub>2</sub>O<sub>4</sub>) has received special attention. Zhang et al. [58] developed a novel magnetic CoFe<sub>2</sub>O<sub>4</sub>-coated TNTs (MTNTs) adsorbent for the removal of heavy metal. The MTNTs are synthesized by a two-step hydrothermal method and CoFe<sub>2</sub>O<sub>4</sub>

Table 4  
Influence of the pH on lead adsorption onto TNTs generated by microwave hydrothermal procedure [56]

pH	Lead adsorption (mmol/g)
2	0.3
3	0.7
4	0.9
5	1.0
6	1.0

Notes: Conditions: 500 mL of solution containing 40 mg/L Pb(II), adsorbent: 20 mg of titanate nanotube generated at 400 W, time: 25 min, and temperature: 25°C.

nanoparticles are successfully incorporated with TNTs, maintaining the tubular structure. The BET surface area of MTNTs was  $218 \text{ m}^2/\text{g}$  and the pore volume  $0.763 \text{ cm}^3/\text{g}$ , a decreased or these are observed it is due to the fact that  $\text{CoFe}_2\text{O}_4$  occupies the partial surface areas of nanotubes. The Pb(II) adsorption over MTNTs is strongly pH dependent. The maximum adsorption capacity of Pb(II) is  $2.1 \text{ mmol/g}$  at pH 5 and decrease sharply to  $0.8 \text{ mmol/g}$  at pH 2. The adsorption of Pb(II) on MTNTs fits better to the Langmuir model. Kinetic studies reveal that the adsorption of Pb(II) on MTNTs is found to be strongly dependent and favored at high pH values. The enhanced Pb(II) adsorption amount with pH can be explained by the surface charge of MTNTs and  $\text{H}^+$  competition for active adsorption sites. The adsorption on Pb(II) onto MTNTs is ionic exchange between Pb(II) and  $\text{Na}^+$  or  $\text{H}^+$  attached to  $\text{Ti}_3\text{O}_7^{2-}$  nanosheets.

Inorganic or organic acids are often used as desorption agents for heavy metal desorption based on the replacement of metal ions by  $\text{H}^+$ . Considering that MTNTs cannot exist stably in the solution at  $\text{pH} < 2$ , saturated EDTA-2Na solution with  $\text{pH} 2.5$  are used for Pb(II) desorption rather than HCl or  $\text{HNO}_3$  solution. In the desorption process using saturated EDTA-2Na the  $\text{H}^+$  in solution and  $\text{Na}^+$  from EDTA-2Na may enter into the interlayer of MTNTs, making Pb(II) unloaded. Then, unloaded Pb(II) is bound to EDTA-2Na as a result of complexation, which hinders the equilibrium between Pb(II) and  $\text{H}^+$  and makes the desorption proceed continuously.

Various divalent cations were used to determine the adsorption properties of sodium TNTs [59]. The metal adsorption is well represented by the Langmuir model, whereas the adsorption order, found at pH 3 and ionic strength of 0.1, is  $\text{Pb} > \text{Cd} > \text{Cu} > \text{Zn} > \text{Ca} > \text{Sr} > \text{Ni}$ , this adsorption capacity can be linked with the hard and soft acids and bases theory, and since these nanotubes showed higher affinities for softer acids, i.e. Pb, Cd, Cu, the sodium TNTs investigated in this work can be considered soft bases.

Titanate nanofibers with  $\text{Na}_x\text{H}_{2-x}\text{Ti}_3\text{O}_7 \cdot n\text{H}_2\text{O}$  (i.e.  $x = 2$ ) were investigated as adsorbents for copper(II) [60]. These nanofibers presented a structure in which three edge-shared  $\text{TiO}_6$  octahedras join at the corners to form stepped and zig-zag  $\text{Ti}_3\text{O}_7^{2-}$  layers; the sodium cations located between the layers can be exchanged with cations. Thus, results concluded that the nanofibers with the higher sodium content are the most effective adsorbents for copper(II), being this adsorption greater as the pH of the solution is increased, reaching a maximum of 99.8% at pH of 4, when a solution of  $100 \text{ mg/L}$  metal were tested; the adsorption follows the Langmuir and the pseudo-second-order models

well. The metal can be desorbed by the use of EDTA- $\text{Na}_2$  solutions, with best results (89.3%) of metal desorption obtained when a  $10^{-1} \text{ M}$  of the desorbent is used.

TNTs with specific surface area of  $272.0 \text{ m}^2/\text{g}$  were used to adsorb lead(II) and cadmium(II) from aqueous solutions [61]. In both cases, the adsorption is related to the hydroxyl groups in the nanotubes. As it is apparently the norm, the adsorption of both metals is pH dependent, increasing with the increase of the aqueous pH value; however, this maximum depends on the metal considered, since the value is 5 for lead (adsorption capacity of more than  $2.2 \text{ mmol/g}$ ) and 4 for cadmium(II) (with a load in the  $1.8 \text{ mmol/g}$  range). Metal recovery from metals loaded nanotubes can be achieved at acidic pH values (i.e. at pH 1, with recoveries of 90% for Cd(II) and 83% for Pb(II)). The adsorptive properties of these TNTs were compared with that of other adsorbents for lead and cadmium (Table 5). It can be seen that with these Ti-based nanoadsorbents, it is achieved the highest metals uptake.

The regeneration of desorbed TNTs prepared by hydrothermal method and dispersed in absolute ethanol was investigated with Cd(II) adsorption and desorption cycles [62]. At pH 5, the maximum adsorption capacity of Cd(II) onto TNTs is  $1.1 \text{ mmol/g}$ , the adsorption equilibrium can be well described by Langmuir models. The adsorption capacity of the TNTs regenerated with  $0.2 \text{ M}$  NaOH solution under ambient conditions rarely decreased during the 6 cycles, and the removal and desorption ( $0.1 \text{ M}$   $\text{HNO}_3$ ) efficiency are above 90%. However, for the TNTs the adsorption and desorption capacity are around 13 and 94%, respectively. After the desorption process, the tubular TNTs structures were almost completely destroyed and transformed into plate structure. However, after regenerated with  $0.2 \text{ M}$  NaOH solution, the sheet-linked TNTs began to roll up towards forming the scroll-type structure, this is due the asymmetric distribution of  $\text{H}^+$  and  $\text{Na}^+$  on the surface side and interlayer region of TNTs plate.

Various forms of titanate nanostructures were used to remove  $\text{Pb}^{2+}$  from aqueous solution [25]. Three types of titanate adsorbents were investigated: nanotubes, nanowires, and amorphous nanoparticles, being in the three cases the metal adsorption fitted to the Langmuir model, thus, the adsorption environment in these titanates derivatives can be viewed as homogeneous system. The adsorption order for the metal is found to be: nanotubes > nanoparticles > nanowires with capacities of near 0.7, 0.5, and  $0.4 \text{ mmol/g}$  for an equilibrium lead concentration of near  $1 \text{ g/L}$ , respectively.

Table 5  
Metal uptake using various adsorbents [61]

Adsorbent	Pb(II) (mmol/g)	Cd(II) (mmol/g)
Activated carbon	0.2	0.2
Titanate nanotubes	2.5	2.1
Manganese oxide coated zeolite	0.3	
Multiwalled carbon nanotubes		0.1

TNTs fabricated by the conventional method of alkaline hydrothermal process and calcined at various temperatures (200–600°C) were used to study the coupled removal of bisphenol A and copper(II) ion [63]. The adsorption mechanism was explained on the basis of the first adsorption of copper ions, these acting as electron traps to reduce recombination rate of  $H^+/e^-$  pairs on the surface of the nanotubes catalysts for photodegradation of bisphenol A. The Langmuir model fitted well the metal adsorption with capacity of 2.5 mmol/g for the non-calcined TNTs, whereas this capacity decreased to 0.6 mmol/g for the nanotubes calcined at 600°C, this is attributed to the decrease in specific surface area of the calcined product, since in the calcination process, anatase nanoparticles were formed on the tube walls to form titania/titanate nanocomposites.

Different TNMs were synthesized via hydrothermal reaction by  $TiO_2$  under 4–15 M NaOH solutions (nanogranules, nanoplates, nanosheets, nanotubes, and nano-blocks) [26]. The adsorption of Cu(II) and Cd(II) on TNMs are strongly affected by the pH. At pH 4 and 5, the adsorption capacity is higher due to increasing negative charges on the surface of TNMs. The pseudo-second-order and Langmuir model could well describe the adsorption kinetics and isotherms, respectively. The maximum capacity adsorption for Cd and Cu onto different TNMs is showed in (Table 6), it is higher to nanosheets and nanotubes. The adsorption mechanism is dominant by the ion-exchange between metal cation and  $Na^+$ , with a less contribution is the ion-exchange between metal cation and  $H^+$  and complexation by  $-OH$ . So the  $Na^+$  content was closely related to the metal adsorption capacity and not the surface area and pore diameter of TNMs.

Titanate nanoflowers have large specific surface area and their performance in the removal of heavy metals were thus investigated; the metals investigated were lead(II) and mixed aqueous solutions of cadmium(II), zinc(II), and nickel(II) [64]. Experimental results showed that the removal order found for these nanocompounds is  $Cd(II) > Zn(II) > Ni(II)$  with maximum adsorption capacities of 0.7, 0.4, and

Table 6  
Maximum capacity adsorption of Cu(II) and Cd(II) (mmol/g), Langmuir isotherm [26]

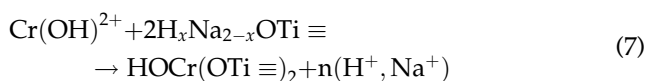
	Cu(II)	Cd(II)
Nanogranules	0.8	0.7
Nanoplates	1.4	1.4
Nanosheets-nanotubes	1.9	1.9
Nanotubes	1.8	1.9
Nanosheets	1.8	1.9
Nano-blocks	1.7	1.8

0.3 mmol/g, respectively, for a metal (each) equilibrium concentration of near 0.17, 0.10, and 0.09 g/L, which is roughly equivalent to  $1.5E-3$  mol/L. The performance of these adsorbents with respect to the metals removal is compared against those of TNTs or nanowires; for each metal, the adsorption capacity follows the next order: nanoflowers > nanotubes > nanowires. With respect to lead(II) adsorption using nanoflowers, adsorption equilibrium is reached within less than 10 min of contact of the aqueous solution and the adsorbent, this quick adsorption is related to the structural characteristics of titanate nanoflowers, where the space between the nanosheets, which formed the nanoflowers, is considered as tunnels which favored the fast diffusion of lead(II) ions; in the present case, the adsorption kinetics can be represented by the pseudo-second-order model, thus, a chemisorption mechanism appeared to be the rate-limiting step. Comparison of lead(II) adsorption using the three nano-adsorbents mentioned above, give the next order: nanoflowers > nanowires > nanotubes.

TNTs with a layered structure were investigated for the uptake of radioactive uranium ions, being this removal performed via an ion exchange process [65]. Metal uptake induces considerable deformation of the layer structures, resulting in a structural change from nanotubes to sheets and the subsequent permanent entrapment of the radioactive cations in the latter.

The adsorption power of TNTs on multi-elemental solutions was investigated in systems containing  $Pb^{2+}$ ,  $Cu^{2+}$ ,  $Cr^{3+}$ , and  $Cd^{2+}$  [66]. From adsorption experiments carried out at an aqueous pH value of 5, the adsorption order and maximum metal loading was:  $Pb^{2+}$  (2.6 mmol/g) >  $Cd^{2+}$  (2.1 mmol/g) >  $Cu^{2+}$  (1.9 mmol/g) >  $Cr^{3+}$  (1.4 mmol/g), whereas the corresponding equilibrium concentrations are: 0.50, 0.10, 0.13, and 0.14 g/L, respectively. The presence of certain ions affected the adsorption of the above metals onto the nanotubes, this adsorption decreases in the presence of  $Ca^{2+}$ ,  $Mg^{2+}$ ,  $K^+$ , and  $Na^+$  due to their competition for adsorption sites, the decrease of the activity of heavy

metals ions, and the promotion of the aggregation of the TNTs which is not beneficial for the adsorption of the heavy metals. In the presence of  $\text{Al}^{3+}$  and  $\text{Fe}^{3+}$ , the adsorption capacity is generally increased due to the formation of hydroxyl-Al/Fe intercalated or coated TNTs which were more effective in the adsorption of the investigated heavy metals. These metals can be desorbed from loaded nanotubes by the use of nitric acid or EDTA, the latter being more effective for desorption. The exception to the above is the case of chromium(III), which is not desorbed with EDTA solutions and only 40% of the metal loaded in the nanotube is recovered with nitric acid; these results are explained in terms of the great stability of the compound formed on reaction of the metal ion with the TNTs:



In the adsorption of Pb(II), Cd(II), and Cr(III) by TNTs [67,68], it was found that the pH of the aqueous solution is the key factor for metal adsorption and the presence of humic acid in this solution also influenced favorably the metal adsorption due to the formation of metal-humic acid complexes which evidently alter the adsorption capacity of the nanotubes. It is worth mentioning that fulvic acid may have a stronger effect on the adsorption of heavy metal ions onto TNTs than humic acid [69]. In the case of the pH, the metal adsorption is enhanced as the pH of the aqueous solution increased from 2 to 6, and follows the order lead>cadmium>chromium; however, at the highest pH value, chromium is adsorbed preferably to cadmium. The presence of humic acid favored metal adsorption at concentration of the acid in the solution below 1 mg/L and above 5 mg/L, whereas between these two limiting values the metal adsorption decays.

TNTs/iron oxide magnetic composites were used to adsorb  $^{109}\text{Cd}(\text{II})$  [70]. This element is the best adsorbed at aqueous pH values in the 7–8 range, being this adsorption related to an outer-sphere or an inner-sphere complexation mechanism depending upon the pH value at which cadmium is removed from the aqueous solution. The presence of humic and fulvic acids in the solution also enhances the adsorption of cadmium onto the adsorbent at pH values lower than 8, but is detrimental for this adsorption at pH values above 9.

The adsorption of cadmium by TNTs was also investigated in the presence of inorganic anions in the solution [71]. In fact, several of these anions (i.e. phosphate, sulfate, and fluoride) are effectively adsorbed

by the nanotubes at aqueous pH values below 4, though this adsorption decreased sharply at pH values above 4. When no anions are presented in aqueous solution, cadmium is effectively adsorbed in the 3.5–8.5 pH range value, and generally the presence of the above anions in the solution decreased the metal adsorption, especially at pH values above 4, whereas cadmium uptake is most affected in the system containing sulfate anions.

Hydrogenotitanates nanotubes,  $\text{H}_x\text{Na}_{2-x}\text{TiO}_5 \cdot \text{H}_2\text{O}$  where  $x$  was 1.61, were prepared by hydrothermal treatment of  $\text{TiO}_2$  followed by washing with HCl aqueous solution to study the adsorption of Pd(II). The BET surface is  $236.0 \text{ m}^2/\text{g}$ . Pd(II) adsorption onto the nanotubes occurred by cationic exchange while above 1.1 mmol/g of deposited Pd(II), then the Pd(II) precipitation occurred [72].

Multilayered TNTs were used to adsorb Cr(III), Cr(VI) of mixtures of both chromium oxidations states [73]. For systems containing only Cr(III), it is found that the maximum metal uptake is 1.1 mmol/g at pH 5, whereas this adsorption is promoted in the presence of Cr(VI) until 1.6 mmol/g at the same pH value. Cr(VI) adsorption from single solutions is negligible at this pH value and only slightly increases (metal uptake of near 0.2 mmol/g) at pH values of near 1. In the presence of Cr(III), the adsorption of Cr(VI) increased until 0.2 mmol/g at the pH of 5. The adsorption of Cr(III) from single solutions can be related to a cation exchange mechanism with the  $\text{Na}^+$  ions in the interlayer of the nanotubes; in the presence of Cr(VI), a more complex mechanism occurred and the element is adsorbed via a double-layer adsorption reaction, in which an ionic cluster of both chromium oxidation states is formed initially and then it is bridged with Cr(III) adsorbed onto the TNTs through Cr(III)-O-Cr(VI) linkages. In the adsorption process, the  $\text{TiO}_6$  structure of the nanotubes is not altered.

Several titanate-based adsorbents were described in the removal of radioactive ions from water [74]. To simulate the removal of  $\text{Ra}^{2+}$  with titanate nanofibers,  $\text{Sr}^{2+}$  and  $\text{Ba}^{2+}$  aqueous solution were used. In the case of strontium(II) and barium(II), the maximum metal uptake is 0.6 mmol/g. In solutions containing 0.25 g/L  $\text{Cs}^+$ , the use of nanotubes can reduce this in an 80%; however, complete metal removal can be obtained when its initial concentration in water is less than 0.08 g/L. The use of titanate nanofibers lowered these percentages, since 36% of the initial 0.13 g/L  $\text{Cs}^+$  is reached when these nanostructures were used as adsorbents. Maximum metal uptakes are near 1.5 and 0.5 mmol/g for nanotubes and nanofibers, respectively, and it is suggested that this variation is due to the larger specific surface area in the former structure



than in the latter one. In all the three above cases, metal uptake cause structural deformations in the titanium-based nanostructures.

Yang et al. [75] demonstrated a potentially cost-effective method to remediate radioactive  $^{131}\text{I}^-$  ions from contaminated water using of TNTs and nanofibers. To capture and immobilize  $\text{I}^-$  ions from water, silver oxide ( $\text{Ag}_2\text{O}$ ) nanocrystals with a size of 5–10 nm were anchored on external surface of TNTs and nanofibers by dispersing them into an aqueous silver nitrate solution. In a neutral or basic suspension ( $\text{pH} \geq 7$ ), most of silver is in the form of  $\text{Ag}_2\text{O}$  nanoparticles and the remainder is in the form of  $\text{Ag}^+$  ions in the interlayer region because of exchange with  $\text{Na}^+$  ions. The author uses stable  $^{125}\text{I}^-$  ions together with radioactive  $\text{I}^-$  ions. The  $^{131}\text{I}^-$  and  $^{125}\text{I}^-$  isotopes have the same chemical reaction properties. Under this condition, nanotubes- $\text{Ag}_2\text{O}$  can reduce over 90% of  $^{125}\text{I}^-$  ions at  $\text{I}^-$  ion concentration below 0.5 g/L, the capacity is 4.5 mmol/g. Similar percentages were obtained by titanate nanofibers- $\text{Ag}_2\text{O}$ , the capacity of nanofibers are slightly lower than nanotubes 3.0 mmol/g.

The adsorption of nickel(II) on TNTs was investigated at various experimental conditions [76,77]. It was found that the adsorption of nickel is pH-dependent, increasing as the pH of the solution increases from 4 to 7 (from near 60% to more than 90%), and both humic and fulvic acids favored the metal uptake, even at the lowest pH value of 4, being this uptake increased as the concentration of the acids in the aqueous solution is increased from nil to 16 g/L. The interaction of the metal with the nanotubes depends of the pH in which this adsorption is carried out. At pH of 4, outer-sphere complexation is the responsible mechanism for nickel adsorption; at pH, 5 both outer and inner-sphere complexes contribute to the adsorption, whereas at pH values above 7, inner-sphere surface complexes, though some precipitation occurs. In the presence of the organic acids, ternary surface complexes can be formed in the nanotubes surface being these responsible of the enhancement of metal adsorption.

The removal of Ni(II) to TNTs is affected by cations in the TNT suspension, 0.01 mol/L  $\text{LiClO}_4$ ,  $\text{NaClO}_4$ , and  $\text{KClO}_4$  at  $\text{pH} < 6$ . The removal percent of Ni(II) to TNT at  $\text{pH} < 6$  follow the next order:  $\text{Li}^+ > \text{Na}^+ > \text{K}^+$ , which indicate that cations can change the surface properties of TNTs and thus influences the adsorption of Ni(II) onto TNTs. The adsorption of Ni(II) to TNTs can be considered as competition of  $\text{Ni}^{2+}$  and  $\text{Li}^+$ ,  $\text{Na}^+$  or  $\text{K}^+$  at the TNT surface. The radius of  $\text{Li}^+$  is larger than those of the other two cations and thus influence of  $\text{Li}^+$  on Ni(II) adsorption to TNTs is smaller than those  $\text{Na}^+$  and  $\text{K}^+$ . However, at  $\text{pH} > 6$  no drastic difference of Ni(II) sorption to TNTs in  $\text{LiClO}_4$ ,  $\text{NaClO}_4$ ,

and  $\text{KClO}_4$  solutions is observed, which may be attributed to the inner-sphere surface complexation or surface precipitates at high pH values. The adsorption of Ni(II) onto TNTs at  $\text{pH} < 6$  in 0.01 mol/L  $\text{NaClO}_4$ ,  $\text{NaNO}_3$ , and  $\text{NaCl}$  solutions is affected by the anions. The removal percent of Ni(II) is lowest in  $\text{NaCl}$  and highest in  $\text{NaClO}_4$  solution [77].

TNTs were also used in calcium(II) and magnesium(II) removal in a continuous form in order to soften water [78]. Some losses in the adsorption capacity was observed after the third cycle, being this capacity loss attributed to the calcium(II) uptake that is apparently strong and irreversible against the reversibility of the magnesium(II)-sodium(I) exchange.

Tl(I) and Tl(III) are the two main oxidation states of thallium, a high toxic element. Tl(I) is the most commonly occurring species of thallium in the most natural environments. Liu et al. [79] examine the adsorption of Tl(I) and Tl(III) on hydrothermally synthesized TNTs  $\text{N}_x\text{H}_{2-x}\text{Ti}_3\text{O}_7 \cdot n\text{H}_2\text{O}$  ( $x = 0-0.75$ , depending on the remaining sodium ions). The surface area of the nanotubes was 272.0  $\text{m}^2/\text{g}$ . Laboratory tests show that the adsorption capacities of Tl(I) and Tl(III) increased with increasing pH. The 100% removal efficiency was achieved when pH is above 5. The optimum pH for Tl(I) adsorption was approximately 5–6, whereas efficient adsorption of Tl(III) was found to occur even at a pH as low as 2 with adsorption capacity 1.9 mmol/g. For solution  $\text{pH} > 3$ , precipitation in the form of  $\text{Tl}(\text{OH})_3$  was the dominant mechanism for Tl(II) removal. The adsorption isotherm of Tl(I) on TNTs fitted closely to the Langmuir isotherm with a calculated maximum adsorption capacity of 3.5 mmol/g. In the case of the adsorption isotherm of Tl(III), neither the Langmuir or Freundlich model in isolation could describe it properly. Instead, the isotherm of Tl(III) on TNTs has two distinct stages at low Tl(III) equilibrium concentration ( $< 10 \text{ mg/L}$ ), the isotherm exhibited a good Langmuir fit. The adsorption was dominated by ion-exchange between Tl(III) ions and  $\text{Na}^+/\text{H}^+$  of TNTs. At high Tl(III) equilibrium concentration (100 mg/L), the adsorption capacity of Tl(III) is dominated by the co-precipitation of Tl(III) onto TNTs. Tl(I) was readily desorbed from TNTs by  $\text{HNO}_3$ , desorption efficiencies were always over 95.0%, ( $\text{HNO}_3$  concentration, 0.2, 0.4, and 0.6 mol/L). The TNTs exhibited a large adsorption capacity for thallium after desorption by  $\text{HNO}_3$  and regeneration by  $\text{NaOH}$ . However, the ratio of adsorption capacity after regeneration to initial capacity decreased to 87.7% when TNTs were desorbed with 0.6 mol/L  $\text{HNO}_3$ , and TNTs could not be fully recovered after  $\text{NaOH}$  treatment. To desorption of Tl(III) from TNTs a solution of  $\text{HNO}_3$  0.4 mol/L is an excellent option.

Table 7

The parameters for Langmuir and Freundlich isotherm model of Eu(III) adsorption onto TNTs at three different temperatures [80]

T (°C)	Langmuir			Freundlich		
	Q <sub>max</sub> (mmol/g)	b (L/mmol)	R <sup>2</sup>	K <sub>F</sub> (mmol <sup>1-n</sup> L <sup>n</sup> /g)	n	R <sup>2</sup>
20	0.123	0.263	0.973	4.98	0.443	0.985
40	0.172	0.264	0.975	6.79	0.375	0.982
70	0.299	0.523	0.975	9.24	0.282	0.972

Eu<sup>3+</sup> is a trivalent lanthanide and a chemical homolog to trivalent radioactive actinides with the similar sorption and ion-exchange properties. Thus, Eu<sup>3+</sup> is used as a representative of ultratoxic radioactive actinides. The adsorption isotherms Eu<sup>3+</sup> onto of the TNTs at temperatures 20, 40, and 70°C can be described by the Freundlich model better than the Langmuir model, Table 7 shows the parameters for both models at different temperatures. The interaction of the Eu(III) with TNTs is mainly controlled by outer-sphere surface complexation at T° = 20°C, which is a reversible adsorption process, whereas at 40 and 70°C Eu(III) interaction is mainly controlled by inner-sphere surface complexation, which is a irreversible adsorption process [80,81].

For the nanosheets, the maximum adsorption capacity for Eu<sup>3+</sup> was 1.7 mmol/g [82]. The adsorption of Ag<sup>+</sup>, Cu<sup>2+</sup>, Pb<sup>2+</sup>, and Eu<sup>3+</sup> (1 mmol/L) by titanate sheet under the presence of large amount of Na<sup>+</sup>, Mg<sup>2+</sup>, and Ca<sup>2+</sup> (200 mmol/L) was studied. Ag<sup>+</sup>, Cu<sup>2+</sup>, Pb<sup>2+</sup>, and Eu<sup>3+</sup> are removed completely due to there being much softer acids than Na<sup>+</sup>, Mg<sup>2+</sup>, and Ca<sup>2+</sup> and thus possessing higher priority in the ion exchange. H<sup>+</sup> (1 mol/L) is used to regenerate the titanates due to the fact that H<sup>+</sup> is the smallest cation and thus may possess the highest priority in the ion exchange.

Black aspergillus/titanate bionanocomposites are investigated as potential radioactive adsorbents for removing radioactive ions from water caused by nuclear disaster [83]. This investigation is carried out using the adsorption of Ba<sup>2+</sup> as a model for the potentially above used, whereas the titanium-based adsorbents are in the nanotube form. Linkage of the fungus with the nanotubes is apparently due to the interactions of the hydroxyl groups of the fungus with Ti–O bonds of the nanotube. Barium uptake is described as high as 0.9 mmol/g. Being the investigation carried out on a non-radioactive water sample, it is unclear the effect of the radioactivity on the fungus and thus the effectiveness of the proposed nanocomposite in the adsorption of the given metals.

### 3. Conclusion

The various tested Ti-based nanostructures certainly presented good properties as adsorbents of metals from aqueous solutions of various sources; however, their application in this environmental field is not fully investigated, since until now, most of the investigations have been performed on synthetic or “ideal” solutions, which is not the real situation when one is faced with an environmental issue. Also, very little information is currently in our hands related with the performance of these nanostructures when used in a continuous operation, i.e. columns, with uncertain problems such as materials attrition, than only the practice lights on. In any case, the future for these nanoadsorbents in this field seemed to be promising and worth to be investigated.

### Acknowledgments

To the CSIC Agency (Spain) for support. And Dra. Irene García-Díaz expresses her gratitude to the Ministry of Economy and Competitiveness for their Postdoctoral Junior Grants (Ref. FPDI-2013-16391).

### References

- [1] Q. Chen, W.Z. Zhou, Trititanate nanotubes made via a single alkali treatment, *Adv. Mater.* 14 (2002) 1208–1211.
- [2] Y.V. Kolen'ko, K.A. Kovnir, A.I. Gavrilo, A.V. Garshev, J. Frantti, O.I. Lebedev, B.R. Churagulov, G. Van Tendeloo, M. Yoshimura, Hydrothermal synthesis and characterization of nanorods of various titanates and titanium dioxide, *J. Phys. Chem. B* 110 (2006) 4030–4038.
- [3] N. Li, L.D. Zhang, Y.Z. Chen, M. Fang, J.X. Zhang, Highly efficient, irreversible and selective ion exchange property of layered titanate nanostructures, *Adv. Funct. Mater.* 22 (2012) 835–841.
- [4] Y. Takezawa, H. Imai, Bottom-up synthesis of titanate nanosheets with hierarchical structures and a high specific surface area, *Small* 2 (2006) 390–393.
- [5] V. Štengl, S. Bakardjieva, J. Šubrt, E. Večerníková, L. Szatmary, M. Klementová, V. Balek, Sodium titanate

- nanorods: Preparation, microstructure characterization and photocatalytic activity, *Appl. Catal. B: Environ.* 63 (2006) 20–30.
- [6] B.X. Wang, Y. Shi, D.F. Xue, Large aspect ratio titanate nanowire prepared by monodispersed titania submicron sphere via simple wet-chemical reactions, *J. Solid State Chem.* 180 (2007) 1028–1037.
- [7] W. Jinxia, L. Wenxia, Y. Guohong, L. Haidong, L. Hong, Z. Weijia, W. Huili, W. Zhe, Delaminated sodium titanate nanobelts in synergy with cationic polyacrylamide to influence flocculation on kaolin clay, *Colloids Surf., A* 414 (2012) 9–16.
- [8] T. Kasuga, M. Hiramatsu, A. Hoson, T. Sekino, K. Niihara, Formation of titanium oxide nanotube, *Langmuir* 14 (1998) 3160.
- [9] T. Kasuga, M. Hiramatsu, A. Hoson, T. Sekino, K. Niihara, Titania nanotubes prepared by chemical processing, *Adv. Mater.* 11 (1999) 1307–1311.
- [10] N. Liu, X. Chen, J. Zhang, J.W. Schwank, A review on TiO<sub>2</sub>-based nanotubes synthesized via hydrothermal method: Formation mechanism, structure modification and photocatalytic applications, *Catal. Today* 225 (2014) 34–51.
- [11] Y.Q. Wang, G.Q. Hu, X.F. Duan, H.L. Sun, Q.K. Xue, Microstructure and formation mechanism of titanium dioxide nanotubes, *Chem. Phys. Lett.* 365(5–6) (2002) 427–431.
- [12] C.-C. Tsai, H. Teng, Regulation of the physical characteristics of titania nanotube aggregates synthesized from hydrothermal treatment, *Chem. Mater.* 16 (2004) 4352–4358.
- [13] H.-K. Seo, G.-S. Kim, S.G. Ansari, Y.-S. Kim, H.-S. Shin, K.-H. Shim, E.-K. Suh, A study on the structure/phase transformation of titanate nanotubes synthesized at various hydrothermal temperatures, *Sol. Energy Mater. Sol. Cells* 92(11) (2008) 1533–1539.
- [14] Y. Inoue, I. Noda, T. Torikai, T. Watari, T. Hotokebuchi, M. Yada, TiO<sub>2</sub> nanotube, nanowire, and rhomboid-shaped particle thin films fixed on a titanium metal plate, *J. Solid State Chem.* 183(1) (2010) 57–64.
- [15] S. Preda, V.S. Teodorescu, A.M. Musuc, C. Andronescu, Influence of the TiO<sub>2</sub> precursors on the thermal and structural stability of titanate-based nanotubes, *J. Mater. Res.* 28 (2013) 294–303.
- [16] Z.H. Li, Z.Q. Liu, Q.Z. Yan, Y.C. Wang, C.C. Ge, Preparation and performance of titanate nanotube by hydrothermal treatment, *Rare Met.* 27 (2008) 187–191.
- [17] D.V. Bavykin, V.N. Parmon, A.A. Lapkin, F.C. Walsh, The effect of hydrothermal conditions on the mesoporous structure of TiO<sub>2</sub> nanotubes, *J. Mater. Chem.* 14 (2004) 3370–3377.
- [18] R. Yoshida, Y. Suzuki, S. Yoshikawa, Effects of synthetic conditions and heat treatment on the structure of partially ion-exchanged titanate nanotubes, *Mater. Chem. Phys.* 91 (2005) 409–416.
- [19] D.V. Bavykin, J.M. Friedrich, F.C. Walsh, Protonated titanates and TiO<sub>2</sub> nanostructured materials: Synthesis, properties, and applications, *Adv. Mater.* 18(21) (2006) 2807–2824.
- [20] W. Zhou, H. Liu, R.I. Boughton, G. Du, J. Lin, J. Wang, D. Liu, One-dimensional single-crystalline Ti–O based nanostructures: Properties, synthesis, modifications and applications, *J. Mater. Chem.* 20 (2010) 5993–6008.
- [21] M.-J. Li, Z.-Y. Chi, Y.-C. Wu, Morphology, chemical composition and phase transformation of hydrothermal derived sodium titanate, *J. Am. Ceram. Soc.* 95 (10) (2012) 3297–3304.
- [22] S. Sreekantan, L.C. Wei, Study on the formation and photocatalytic activity of titanate nanotubes synthesized via hydrothermal method, *J. Alloys Compd.* 490 (1–2) (2010) 436–442.
- [23] Z.-Y. Yuan, B.L. Su, Titanium oxide nanotubes, nanofibers and nanowires, *Colloids Surf., A* 241 (2004) 173–183.
- [24] E. Morgado, A.S. de Abreu, G.T. Moure, B.A. Marinkovic, P.M. Jardim, A.S. Araujo, Characterization of nanostructured titanates obtained by alkali treatment of TiO<sub>2</sub>-anatases with distinct crystal size, *Chem. Mater.* 19(4) (2007) 665–676.
- [25] J. Huang, Y. Cao, Z. Deng, H. Tong, Formation of titanate nanostructures under different NaOH concentration and their application in wastewater treatment, *J. Solid State Chem.* 184(3) (2011) 712–719.
- [26] W. Liu, W. Sun, Y. Han, M. Ahmad, J. Ni, Adsorption of Cu(II) and Cd(II) on titanate nanomaterials synthesized via hydrothermal method under different NaOH concentrations: Role of sodium content, *Colloids Surf., A* 452 (2014) 138–147.
- [27] Y.F. Chen, C.Y. Lee, M.Y. Yeng, H.T. Chiu, Preparing titanium oxide with various morphologies, *Mater. Chem. Phys.* 81(1) (2003) 39–44.
- [28] D.V. Bavykin, B.A. Cressey, M.E. Light, F.C. Walsh, An aqueous, alkaline route to titanate nanotubes under atmospheric pressure conditions, *Nanotechnology* 19 (27) (2008) 275604.
- [29] R. Ma, K. Fukuda, T. Sasaki, M. Osada, Y. Bando, Structural features of titanate nanotubes/nanobelts revealed by Raman, X-ray absorption fine structure and electron diffraction characterizations, *J. Phys. Chem. B* 109(13) (2005) 6210–6214.
- [30] P. Dong, B. Liu, Y. Wang, L. Guo, Y. Huang, S. Yin, A study on the H<sub>2</sub>Ti<sub>3</sub>O<sub>7</sub> sheet-like products during the formation process of titanate nanotubes, *J. Electrochem. Soc.* 158 (2011) K183–K186.
- [31] Y. Zhong-Yong, C. Jean Francois, S. Bao-Lian, Titanium oxide nanoribbons, *Chem. Phys. Lett.* 363 (2002) 36–3266.
- [32] Y. Zhong-Yong, S. Bao-Lian, Titanium oxide nanotubes, nanofibers and nanowires, *Colloids Surf., A* 241 (2004) 173–183.
- [33] Y. Lan, X.P. Gao, H.Y. Zhu, Z.F. Zheng, T.Y. Yan, F. Wu, S.P. Ringer, Titanate nanotubes and nanorods prepared from rutile powder, *Adv. Funct. Mater.* 15(8) (2005) 1310–1318.
- [34] E. Horváth, A. Kukovecz, Z. Kónya, I. Kiricsi, Hydrothermal conversion of self-assembled titanate nanotubes into nanowires in a revolving autoclave, *Chem. Mater.* 19(4) (2007) 927–931.
- [35] R. Yoshida, Y. Suzuki, S. Yoshikawa, Syntheses of TiO<sub>2</sub> (B) nanowires and TiO<sub>2</sub> anatase nanowires by hydrothermal and post-heat treatments, *J. Solid State Chem.* 178 (2005) 2179–2185.
- [36] C.-H. Lee, K.-S. Lin, C.-F. Wu, M.-D. Lyu, C.-C. Lo, Effects of synthesis temperature on the microstructures and basic dyes adsorption of titanate nanotubes, *J. Hazard. Mater.* 150 (2008) 494–503.

- [37] J.Q. Huang, Y.G. Cao, Q.F. Huang, H. He, Y. Liu, W. Guo, M.C. Hong, High-temperature formation of titanate nanotubes and the transformation mechanism of nanotubes into nanowires, *Cryst. Growth Des.* 9(8) (2009) 3632–3637.
- [38] C.-C. Tsai, H. Teng, Structural features of nanotubes synthesized from NaOH treatment on TiO<sub>2</sub> with different post-treatments, *Chem. Mat.* 18(2) (2006) 367–373.
- [39] C.-K. Lee, C.-C. Wang, M.-D. Lyu, L.-C. Juang, S.-S. Liu, S.-H. Hung, Effects of sodium content and calcination temperature on the morphology, structure and photocatalytic activity of nanotubular titanates, *J. Colloid Interface Sci.* 316 (2007) 562–569.
- [40] E. Morgado, A.S. de Abreu, R.C. Pravia, B.A. Marinkovic, P.M. Jardim, F.C. Rizzo, A.S. Araújo, A study on the structure and thermal stability of titanate nanotubes as a function of sodium content, *Solid State Sci.* 8 (2006) 888–900.
- [41] C.Y. Liu, L. Miao, R. Huang, S. Tanemura, Effect of different washing treatments on the formation of titanate nanotubes, *Mater. Sci. Forum.* 663–665 (2011) 1247–1251.
- [42] W. Li, T. Fu, F. Xie, S. Yu, S. He, The multi-staged formation process of titanium oxide nanotubes and its thermal stability, *Mater. Lett.* 61 (2007) 730–735.
- [43] B.F. Leo, K.H. Tan, M.N. Ng, C.A. Bee, R.J. Mohd, Physico-chemical properties of titania nanotubes synthesized via hydrothermal and annealing treatment, *Appl. Surf. Sci.* 258 (2011) 431–435.
- [44] L. Xiong, Y. Yang, J.X. Mai, W.L. Sun, C.Y. Zhang, D.P. Wei, Q. Chen, J. Ni, Adsorption behavior of methylene blue onto titanate nanotubes, *Chem. Eng. J.* 156 (2010), 313–320.
- [45] Q. Zhao, M. Li, J.Y. Chu, T.S. Jiang, H.B. Yin, Preparation, characterization of Au (or Pt)-loaded titania nanotubes and their photocatalytic activities for degradation of methyl orange, *Appl. Surf. Sci.* 255 (2009) 3773–3778.
- [46] Y.P. Peng, S.L. Lo, H.H. Ou, S.W. Lai, Microwave-assisted hydrothermal synthesis of N-doped titanate nanotubes for visible-light-responsive photocatalysis, *J. Hazard. Mater.* 183 (2010) 754–758.
- [47] R.A. Doong, L.F. Chiang, Coupled removal of organic compounds and heavy metals by titanate/carbon nanotube composites, *Water Sci. Technol.* 58(10) (2008) 1985–1992.
- [48] H.-Q. An, B.-L. Zhu, H.-Y. Wu, M. Zhang, S.-R. Wang, S.-M. Zhang, S.-H. Wu, W.-P. Huang, Synthesis and characterization of titanate and Cs<sub>2</sub>-modified titanate nanotubes as well as their adsorption capacities for heavy metals ions, *Gaodeng Xuexiao Huaxue Xuebao/Chem. J. Chin. U* 29(3) (2008) 439–444.
- [49] S.-S. Liu, C.-K. Lee, H.-C. Chen, C.-C. Wang, L.-C. Juang, Application of titanate nanotubes for Cu(II) ions adsorptive removal from aqueous solution, *Chem. Eng. J.* 147 (2009) 188–193.
- [50] H.Y. Niu, J.M. Wang, Y.L. Shi, Y.Q. Cai, F.S. Wei, Adsorption behavior of arsenic onto protonated titanate nanotubes prepared via hydrothermal method, *Microporous Mesoporous Mater.* 122 (2009) 28–35.
- [51] R. Mu, Z. Xu, L. Li, Y. Shao, H. Wan, S. Zheng, On the photocatalytic properties of elongated TiO<sub>2</sub> nanoparticles for phenol degradation and Cr(VI) reduction, *J. Hazard. Mater.* 176 (2010) 495–502.
- [52] L. Yang, Y. Xiao, S. Liu, Y. Li, Q. Cai, S. Luo, G. Zeng, Photocatalytic reduction of Cr(VI) on WO<sub>3</sub> doped long TiO<sub>2</sub> nanotube arrays in the presence of citric acid, *Appl. Catal., B* 94 (2010) 142–149.
- [53] W. Liu, J. Ni, X. Yin, Synergy of photocatalysis and adsorption for simultaneous removal of Cr(VI) and Cr(III) with TiO<sub>2</sub> and titanate nanotubes, *Water Res.* 53 (2014) 12–25.
- [54] Y. Hang, H. Yin, A. Wang, Preparation of titanate whiskers starting from metatitanic acid and their adsorption performances for Cu(II), Pb(II), and Cr(III) ions, *Water Air Soil Pollut.* 225 (2014) 2095–2109.
- [55] Y. Chang, S. Xing, X. Wei, Y. Wu, Z. Ma, Lignosulfonate-assisted hydrothermal method for synthesis of titanate nanotubes with improved adsorption capacity for metal ions, *Mater. Lett.* 132 (2014) 353–356.
- [56] Y.-C. Chen, S.-L. Lo, J. Kuo, Pb(II) adsorption capacity and behavior of titanate nanotubes made by microwave hydrothermal method, *Colloids Surf., A* 361 (2010) 126–131.
- [57] J. Wang, S. Zheng, Y. Shao, J. Liu, Z. Xu, D. Zhu, Amino-Functionalized Fe<sub>3</sub>O<sub>4</sub>@SiO<sub>2</sub> core-shell magnetic nanomaterials as a novel adsorbent for aqueous heavy metals removal, *J. Colloid Interface Sci.* 349 (2010) 293–299.
- [58] L. Zhang, X. Wang, H. Chen, F. Jiang, Adsorption of Pb(II) using magnetic titanate nanotubes prepared via two-step hydrothermal method, *Clean—Soil, Air, Water* 42(7) (2014) 947–955.
- [59] A.J. Du, D.D. Sun, J.O. Leckie, Selective sorption of divalent cations using a high capacity sorbent, *J. Hazard. Mater.* 187 (2011) 96–100.
- [60] N. Li, L. Zhang, Y. Chen, Y. Tian, H. Wang, Adsorption behavior of Cu(II) onto titanate nanofibers prepared by alkali treatment, *J. Hazard. Mater.* 189 (2011) 265.
- [61] L. Xiong, C. Chen, Q. Chen, J. Ni, Adsorption of Pb(II) and Cd(II) from aqueous solutions using titanate nanotubes prepared via hydrothermal method, *J. Hazard. Mater.* 189 (2011) 741–748.
- [62] T. Wang, W. Liu, N. Xu, J. Ni, Adsorption and desorption of Cd(II) onto titanate nanotubes and efficient regeneration of tubular structures, *J. Hazard. Mater.* (2013) 250–251.
- [63] R.-A. Doong, C.-W. Tsai, C.-I. Liao, Coupled removal of bisphenol A and copper ion by titanate nanotubes fabricated at different calcination temperatures, *Sep. Purif. Technol.* 91 (2012) 81–88.
- [64] J. Huang, Y. Cao, Z. Liu, Z. Deng, F. Tang, W. Wang, Efficient removal of heavy metal ions from water system by titanate nanoflowers, *Chem. Eng. J.* 180 (2012) 75–80.
- [65] M. Xu, G. Wei, S. Li, X. Niu, H. Chen, H. Zhang, M. Chubik, A. Gromov, W. Han, Titanate nanotubes as a promising adsorbent for high effective radioactive uranium ions uptake, *J. Nanosci. Nanotechnol.* 12(8) (2012) 6374–6379.
- [66] W. Liu, T. Wang, A.G.L. Borthwick, Y. Wang, X. Yin, X. Li, J. Ni, Adsorption of Pb<sup>2+</sup>, Cd<sup>2+</sup>, Cu<sup>2+</sup> and Cr<sup>3+</sup> onto titanate nanotubes: Competition and effect of inorganic ions, *Sci. Total Environ.* 456–457 (2013) 171–180.
- [67] T. Wang, W. Liu, L. Xiong, N. Xu, J. Ni, Influence of pH, ionic strength and humic acid on competitive adsorption of Pb(II), Cd(II) and Cr(III) onto titanate nanotubes, *Chem. Eng. J.* 215–216 (2013) 366–374.

- [68] W.-W. Tang, G.-M. Zeng, J.-L. Gong, J. Liang, P. Xu, C. Zhang, B.-B. Huang, Impact of humic/fulvic acid on the removal of heavy metals from aqueous solutions using nanomaterials: A review, *Sci. Total Environ.* 468–469 (2014) 1014–1027.
- [69] G.D. Sheng, S.T. Yang, J. Sheng, D.L. Zhao, X.K. Wang, Influence of solution chemistry on the removal of Ni(II) from aqueous solution to titanate nanotubes, *Chem. Eng. J.* 168(1) (2011) 178–182.
- [70] L. Dai, L.J. Zheng, L. Wang, Fabrication of titanate nanotubes/iron oxide magnetic composite for the high efficient capture of radionuclides: A case investigation of  $^{109}\text{Cd}(\text{II})$ , *J. Radioanal. Nucl. Chem.* 298 (2013) 1947–1956.
- [71] L. Zhang, A.J. Du, D.D. Sun, J.O. Leckie, Effects of inorganic anions on cadmium sorption behaviours on titanate nanotube surfaces, *Environ. Technol.* 34 (2013) 3017–3021.
- [72] H. Kochkar, A. Turki, L. Bergaoui, G. Berhault, A. Ghorbel, Study of Pd(II) adsorption over titanate nanotubes of different diameters, *J. Colloid Interface Sci.* 331 (2009) 27–31.
- [73] W. Liu, H. Chen, A.G.L. Borthwick, Y. Han, J. Ni, Mutual promotion mechanism for adsorption of coexisting Cr(III) and Cr(VI) onto titanate nanotubes, *Chem. Eng. J.* 232 (2013) 228–236.
- [74] D. Yang, H. Liu, Z. Zheng, S. Sarina, H. Zhu, Titanate-based adsorbents for radioactive ions entrapment from water, *Nanoscale* 5 (2013) 2232–2242.
- [75] D. Yang, S. Sarina, H. Zhu, H. Liu, Z. Zheng, M. Xie, S.V. Smith, S. Komarneni, Capture of radioactive cesium and iodide ions from water by using titanate nanofibers and nanotubes, *Angew. Chem. Int. Ed.* 50 (2011) 10594–10598.
- [76] G. Sheng, L. Ye, H. Dong, H. Li, X. Gao, Y. Huang, EXAFS study of the interfacial interaction of nickel(II) on titanate nanotubes: Role of contact time, pH and humic substances, *Chem. Eng. J.* 248 (2014) 71–78.
- [77] G. Sheng, S. Yang, J. Sheng, D. Zhao, S. Wang, Influence of solution chemistry on the removal of Ni(II) from aqueous solution to titanate nanotubes, *Chem. Eng. J.* 168 (2001) 178–182.
- [78] D. Madarász, I. Szent, A. Sápi, J. Halász, Ákos Kukovecz, Z. Kónya, Exploiting the ion-exchange ability of titanate nanotubes in a model water softening process, *Chem. Phys. Lett.* 591 (2014) 161–165.
- [79] W. Liu, P. Zhang, A.L. Borthwick, H. Chen, J. Ni, Adsorption mechanisms of thallium(I) and thallium(III) by titanate nanotubes: Ion-exchange and co-precipitation, *J. Colloid Interface Sci.* 423 (2014) 67–75.
- [80] G.D. Sheng, S.T. Yang, D.L. Zhao, J. Sheng, X.K. Wang, Adsorption of Eu(III) on titanate nanotubes studied by a combination of batch and EXAFS technique, *Sci. China-Chem.* 55 (2012) 182–194.
- [81] G. Sheng, H. Dong, R. Shen, Y. Li, Microscopic insights into the temperature-dependent adsorption of Eu(III) onto titanate nanotubes studied by FTIR, XPS, XAFS and batch technique, *Chem. Eng. J.* 217 (2013) 486–494.
- [82] N. Li, L. Zhang, Y. Chen, M. Fang, J. Zhang, H. Wang, Highly efficient, irreversible and selective ion exchange property of layered titanate nanostructures, *Adv. Funct. Mater.* 22 (2012) 835–841.
- [83] M. Xu, G. Wei, N. Liu, L. Zhou, C. Fu, M. Chubik, A. Gromov, W. Han, Novel fungus-titanate bio-nanocomposites as high performance adsorbents for the efficient removal of radioactive ions from wastewater, *Nanoscale* 6 (2014) 722–725.